Universitat Autònoma de Barcelona

MELISSA collaboration agreement ECT/FG/CB/95.205

ESTEC/CONTRACT11549/95/NL/FG

- TECHNICAL NOTE 25.110-

IV Compartment, High dilution rate tests

Version : 1

Issue : 0

VERNEREY A. ; ALBIOL J. ; GODIA F.

Dpt. Enginyeria Química

Universitat Autònoma de Barcelona

08193 Bellaterra, Barcelona, Spain

JULY 1996

INTRODUCTION

The previous compartment IV studies allowed the development of a mathematical model describing the behaviour of the Spirulina cultures in front of different radiant fluxes. This mathematical model has later been used in the development of a simulator program (PHOTOSIM) and also a control program that is used in the GPS station. The model has been validated, in the framework of the MELISSA experimental conditions, for low dilution rate experimental protocols. In the next step the model has to be confronted with new experimental data obtained under higher dilution rate test conditions. The present technical note describes the results obtained at two higher dilution rate experimental conditions.

Previous to the realisation of the tests, biomass and light sensors have been re-calibrated. The procedure followed is also described in this technical note.

BIOMASS SENSOR RE-CALIBRATION

The biomass sensor used in the current implementation of compartment IV consists in an in-situ sterilizable probe (Monitek), that measures the absorbance at 746 nm of the culture media. At this wave length, the possible influence of the absorbance due to some cell components like the photosynthetic pigments is minimised. Therefore the absorbance measured is mainly due to the biomass particles. It is assumed also that there is no influence of the exopolysaccharide on this measurement because it does not absorb at this wavelength. However the change in exopolysaccharide concentration might influence the measurement by other mechanisms like by changing the mean refractive index of the biomass particles or by changing the characteristic size of the micro-organism. At this moment it is assumed that this effects on the measurement are of a magnitude small enough to be considered negligible. Future results will allow to more properly asses this point.

Due to the fact that the lamp contained inside of this sensor was changed prior the removal of the equipment from ESTEC, a re-calibration of the sensor was required.

Very few references can be found in the previous technical notes describing the way this important sensor was calibrated before. On CCN5 final report, C. Binois states that this sensor was calibrated by a correlation between the signal given by the sensor and the amount of biomass concentration determined by parallel measures of "dry weight". The biomass determined in this way was named active biomass and referred as C_{XA}. At present time the tern "active biomass" is used to define the biomass devoid of any glycogen and exopolysaccharide.

The biomass concentration determined using this probe is directly used by the GPS program to determine the Fr and the productivity. Therefore in the sensor re-calibration procedure we also have to take this fact into account.

To calculate the Fr the GPS program makes use of a mathematical model which in its first version, actually the one used in the GPS, was not considering different stoichiometries for the biomass and external polysaccharide production. Therefore the external exopolysaccharide is implicitly considered in the active biomass. The model takes into account the possibility of glycogen production but the corresponding parameter is actually set to zero because it is assumed that glycogen is only produced under mineral limitation, which is not the case in the current experimental protocols. In consequence, for the GPS implementation currently used, the active biomass and the total biomass determined with dry weight measurements, are numerically equivalent.

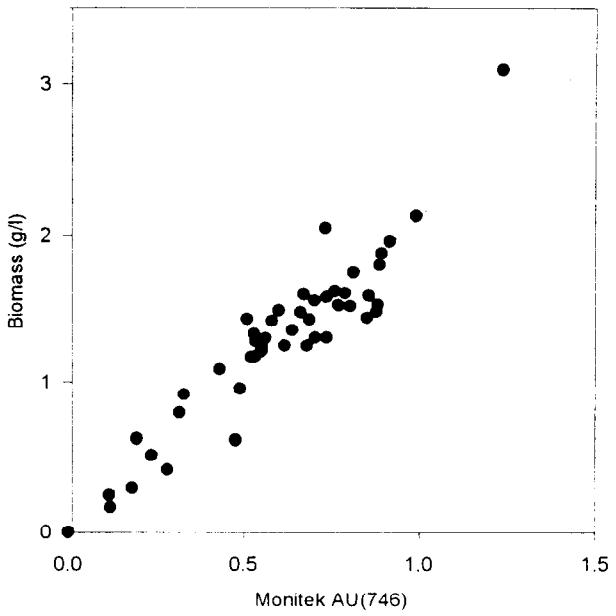

Figure 1: Biomass determined using dry weight of filtered samples

The value given by the sensor is also used by the GPS to calculate the productivity. Also in this case the productivity is calculated directly using the biomass determined by the probe, and therefore considering active biomass and total biomass numerically equivalent. According to this GPS implementation, the first approximation taken for the biomass sensor calibration was to determine the total biomass by the measurement of the dry weight of samples obtained under different working conditions. This values were correlated with the corresponding sensor readings in order to obtain the appropriate relationship between the sensor reading and biomass concentration. The results of this correlation are presented in figure 1 and table 2.

Figure 2: Biomass determined using spectrophotometric measurements and a calibration curve.

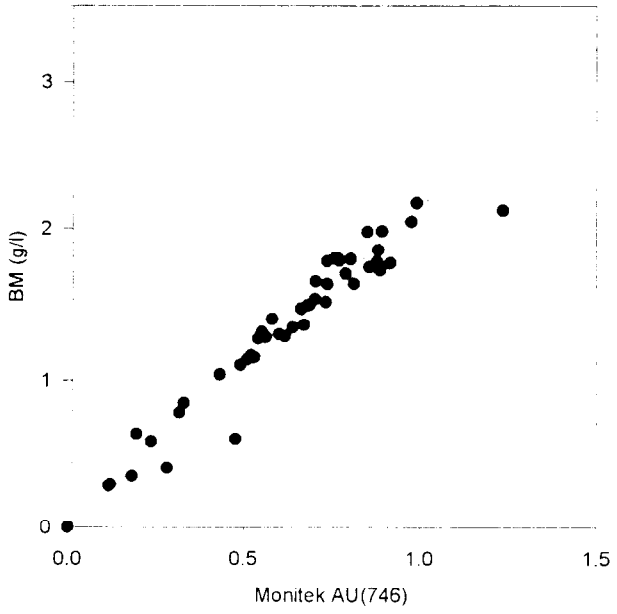

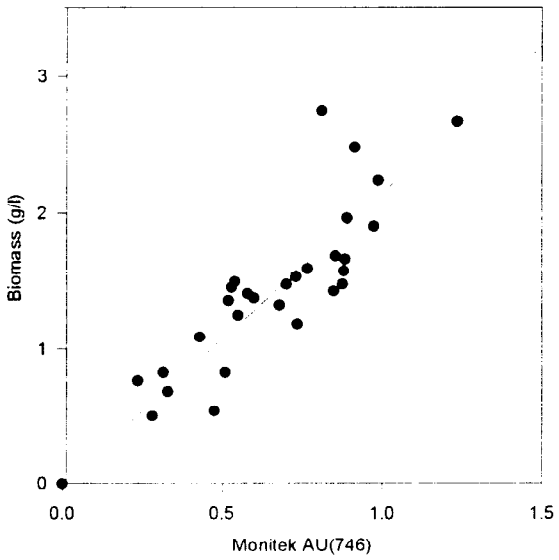

Figure 3: Biomass determined using freeze dried samples

It was also determined, for the same samples, the spectrophotometric absorbance readings at 750 nm and the values converted to active biomass using the correlation given by Thauvoye (Thauvoye 1994), which relates this spectrophotometric readings with the active biomass in the Kontron spectrophotometer used.

The correlation among this determined biomass and the biomass probe readings can be seen in figure 2 and table 2. During the measuring it was also possible to determine the dry weight of freeze dried biomass and the results can be seen in table 2 and in figure 3 correlated with the corresponding biomass probe readings. The figures show that a straight line can be used for a correlation in the range of concentrations used. It can also be seen that the scattering of the measurements around the straight line is higher in the case of the freeze dried biomass. This is probably due to the fact that more manipulations are needed to obtain the freeze dried samples and therefore there are looses in the precision of the dry weight determination.

Figure 4: Relationship among incident light flux Fr and % exopolysaccharide according TN-19.2

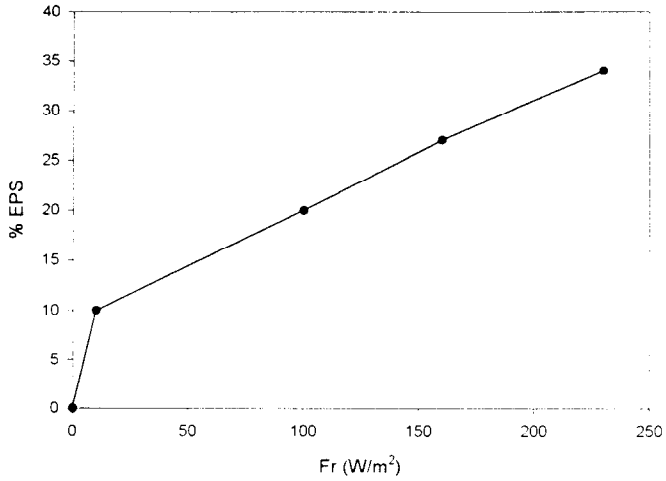

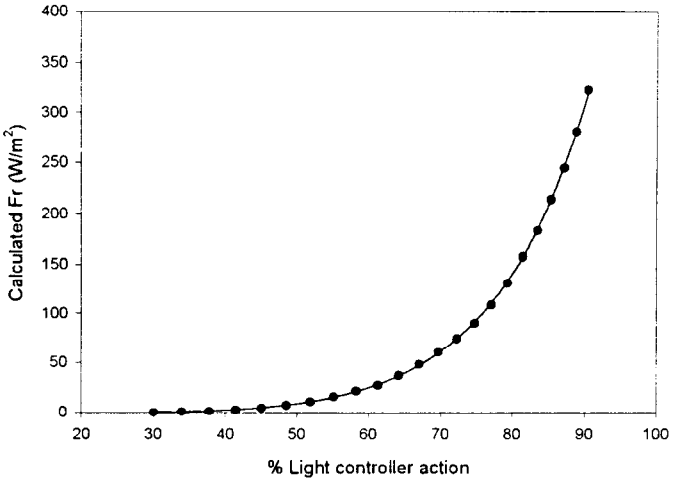

Figure 5 : Plot of the Fr values calculated in front of the % action of the light controller

Due to the fact that the quantity of exopolysaccharide produced varies depending on the illumination conditions it can be discussed that the calibration of the sensor has to be done for each illumination condition. In this work this is not appropriate, due to the fact that the experimental procedure implies to work with at different illumination conditions in order to test the dynamic behaviour of the system. Moreover, the GPS controls the productivity by changing the illumination conditions. In conclusion the use of a calibration of the sensor based on total biomass will always give only an approximation of the real total biomass produced. Therefore another approximation has to be found.

The fact that the biomass sensor measures the absorbance at a wavelength in which the exopolysaccharide does not absorb can be used to measure the "active biomass" and to estimate the total biomass by using the mathematical model. An update of the mathematical model that takes into account in a different way the active biomass and the exopolysaccharide production was already presented by Cornet in TN-19.2 which supplied an update of the equations and coefficients to use in the new model. The implementation of that mathematical model on the GPS would allow to take the "active biomass" measurement and using the information of the illumination conditions given by the light sensor, calculate the exopolysaccharide production and therefore the total biomass production could be obtained. As this model has not yet been implemented on the GPS the percentage of the exopolysaccharide could be estimated using a correlation given by Cornet and depicted in figure 4.

This correlation among Fr and the percentage of exopolysaccharide production may allow to supply to the GPS an approximation of the total biomass that can be used to calculate the Fr and the productivity with the actual model. Of course, as the percentage of EPS is obtained using an average (between the low and high light intensities user in the experiment) of the Fr going to be used in the real experiment, only an approximation of the real biomass values will be obtained. This will probably underestimate the exopolysaccharide content under high illumination conditions and overestimate it under the lower illumination. The result of this will also be an approximation for the productivity and for the Fr calculated by the GPS.

TEST	A	B	C	D	E	F	G	H
Dil. Rate	0.025	0.025	0.025	0.025	0.035	0.035	0.035	0.035
% light Ctrl. Action.	75	85	75	85	75	85	75	85
Fr (calc) (W/m^2)	100	200	100	200	100	200	100	200
Monitech AU	0.548	0.573	0.454	0.585	0.329	0.436	0.345	0.433
Total Bm (g/l)	1.03	1.18	0.91	1.13	0.66	0.92	0.66	0.89
S.D.	0.09	0.04	0.06	0.06	0.02	0.02	0.02	0.02
Active Bm (g/l)	0.72	0.95	0.69	0.96	0.50	0.63	0.46	0.61
S.D.	0.09	0.05	0.07	0.02	0.02	0.015	0.02	0.02

Table 1 : Values of the steady state data used for the biomass probe calibration in active biomass .

According to TN-19.2 as the model currently used in the GPS was unable to predict the deviations produced by the exopolysaccharide production, the model parameters were adjusted assuming a constant exopolysaccharide production of 20%. Therefore the actual GPS Fr predictions will only be the correct ones when the biomass has indeed 20% of EPS. This corresponds to an Fr of about 100 W/m^2 according to the previous Cornet results. As this is one of our calculated illumination conditions, one possibility is to calibrate the biomass sensor for biomass with 20% of exopolysaccharide. In this case, although the predictions of Fr for the biomass with 20% of polysaccharide can be accurate, it will underestimate the total biomass for the biomass composition of higher EPS content. This will cause a false prediction of the Fr because the sensor will receive a smaller light intensity than it corresponds for the biomass quantity value it also receives.

For all it has been said, and in view of future improvements on the GPS, it appears that a second sensible option is to calibrate the biomass sensor to give active biomass, devoid of any polysaccharide. But as at present time the GPS needs a value corresponding to total biomass, the EPS production has to be approximated by another method, and the active biomass converted to total biomass depending on the EPS production. To do this alternative calibration, a way of measuring the EPS or the active biomass has to be available.

After several conversations with J.F. Cornet, about the way the EPS can be determined and also about the measurements needed to check the validity of the model at this high dilution rates, it was concluded that a good compromise between the accuracy of the method used and the time to obtain the results would be to measure, off-line, the total carbohydrate content of the biomass and, taking into account a content of 15% of the of the total biomass as the carbohydrates usually contained in the active biomass, to calculate the values of EPS and active biomass. This determination together with the measure of total biomass and protein content, will allow the assessment of model validity at high dilution rates. The active biomass values determined during this tests can be used to calibrate the biomass sensor as giving the value of "active biomass". As soon as more

measurements are being available, this method will allow to also asses if the changes in illumination (or EPS content) affect the scattering behaviour in a significant way, and therefore if it can be used in the future for the active biomass estimation. For this reasons the values of active biomass obtained during this high dilution tests have been used to calibrate the sensor as measuring "active biomass". A correction to approximate the total biomass as a value for the GPS can later be applied depending on the illumination conditions.

For each sample taken at steady state for the high dilution rate tests, the total carbohydrates were determined and the active biomass calculated. The values obtained of this measurements, for each illumination conditions, were averaged and the standard deviations calculated (table 1). At the same time the absorbance values measured by the MoniteK were recorded and averaged.

In the range of concentrations used up to now (0-2. g/l) it has been shown that the values obtained can be used to calibrate the sensor using a straight line. As the sensor is set to zero using the culture media, before starting any new culture, the value of the readings without biomass are always zero, and therefore for the calibration it is only necessary to obtain the slope of the straight line. As more values are obtained in the future the accuracy of the straight line calibration approximation can be reassessed. The values used for the calibration factor calculation can be found in table 1. With those values a calibration factor of 1.5 +/- 0.05 for the active biomass and a value of 1.99 +/- 0.03 for total biomass can be calculated.

The Fr values to use can also obtained using an estimation done by J.F. Cornet using previous results obtained by C. Binois in the Spirulina air-lift. This correlation relates the watts consumed by the lamps to the Fr according to the equation :

$$Fr = (W)^2 * 0.82$$

Where W stands for the watts consumed by one lamp. To obtain this value a lamp was tested under different voltages and the intensity in Amps was recorded for each voltage. The product of this two values gives the watts consumed by the lamp. With this values a correlation among the voltage supplied to the lamps and the Fr is obtained. The

Table 2 :Summary of the different slope coefficients found in different tests for the biomass sensor calibration.

	SLOPE COEFFICIENT	S.D.
Total biomass (filtered samples)	2.12	0.04
Total biomass (Spectrophotometer)	2.14	0.03
Total biomass (Freeze dried samples)	2.15	0.07
Total biomass (high dilution tests)	1.99	0.03
Active biomass (high dilution tests)	1.5	0.05

relation among the controller action on the supplied voltage is also known, therefore this values allow us to estimate the Fr from the value of the action of the controller. The results can be seen in Figure 5. This method has been used for Fr estimation in this technical note during the period in which the light sensor had to be repaired.

LIGHT SENSOR RECALIBRATION

During the first tests done using the GPS it was observed that the Fr values calculated were higher than the expected ones. Since in the version 2.1 of the GPS there is a new high limit for the Fr calculated by this program set at 400 W/m^2. The GPS reached this top value for what really was a smaller light intensity and therefore it was unable to increase the light intensity up to the real values. As a consequence the biomass level could not increase to the desired concentration. The effect is similar to the one that can be observed in the lasts experiments done at ESTEC (Tn.24.2 ; fig.10) where it can be seen that the Eb values given by the sensor for the current biomass level allow to calculate Fr values higher than 400 W/m^2. However by that time the high limit for the Fr was 8000 W/m^2 and the GPS could continue its control and increase the light to obtain the desired biomass level.

Upon checking the system a software problem was discarded by comparing the Fr values given by GPS with the ones obtained using Matlab and the ADERSA supplied functions. On the other hand it was calculated the Eb that the sensor should give for the real biomass and light intensity used and it was observed that the value was higher than it should have been.

On checking the light amplifier it was observed that not only the values given by this sensor, compared with the values given by an equal sensor of the same type but for a flat surface were higher but also that when the light intensity decreased to the levels of the lower amplifier scale, negative voltage values were obtained on crossing the second scale to the first scale (-6V). It was also observed that, once the amplifier was at the first scale, the output voltage values obtained were first positive and progressively became negative at half the scale. Up on consulting with the ESA technical officer it was decided to send the sensor to ESTEC for repairing.

Once the sensor was back the readings on the first scale had been improved, however the negative peak of voltage (-6V) is still obtained. This peak is converted to 0 by the voltage to current converters, so the controller input values fall to 0 when

Table 3 : Light intensity values measured on two planes separated 1 cm, and used for light sensor calibration. Values are expressed in µmol.m^2.s .

PLANE	A					B				
Position	-2	-1	0	1	2	-2	-1	0	1	2
-2	17.5	17.4	17.6	17.4	17.2	17.5	17.0	16.9	16.8	16.5
-1	17.8	17.7	17.7	17.5	17.3	17.4	17.3	17.15	17.1	16.9
0	18.7	18.2	18.1	17.7	17.6	17.8	17.6	17.5	17.1	17.0
1	18.3	17.16	18.1	17.7	17.6	17.8	17.6	17.6	17.2	17.1
2	18.4	18.2	18.2	17.9	17.7	17.9	17.74	17.7	17.4	17.3
Average	17.8 +/- 0.3					17.3 +/- 0.2				

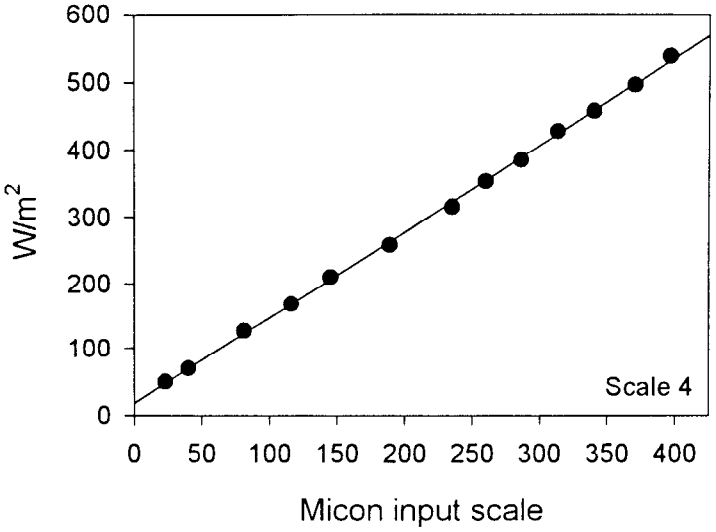

Figure 6 : Calibration plot for light sensor scale 4. (W/m^2= 18.57+1.295* INPUT) .

changing from the second to the first scale. This fact takes place at the same time that all the digital outputs of the amplifier are set to the ON state. This digital outputs are, in normal conditions, set to ON only one at each time and indicate which amplifier scale is being used. The fact that more than one digital input is set to ON when changing from the second scale to the first scale, is used to filter the fall to zero values when changing the amplifier scale.

As some pieces of the amplifier have been changed during the repairing, a new calibration had to be performed on the light sensor, prior to its use. On the technical notes it can be found that this sensor has been calibrated two times. On a first occasion (TN-18.2) the sensor was calibrated at the XAO department at ESTEC using a special set up (a light sensor measuring between 360-1100 nm and a 400-700 filter) prepared on purpose. After that first calibration, some modifications were done to expand the measuring range of the sensor, and the sensor was re-calibrated again (TN-18.2). This

Figure 7 : Calibration plot for light sensor scale 3. (W/m^2= 2.88+0.1254* INPUT).

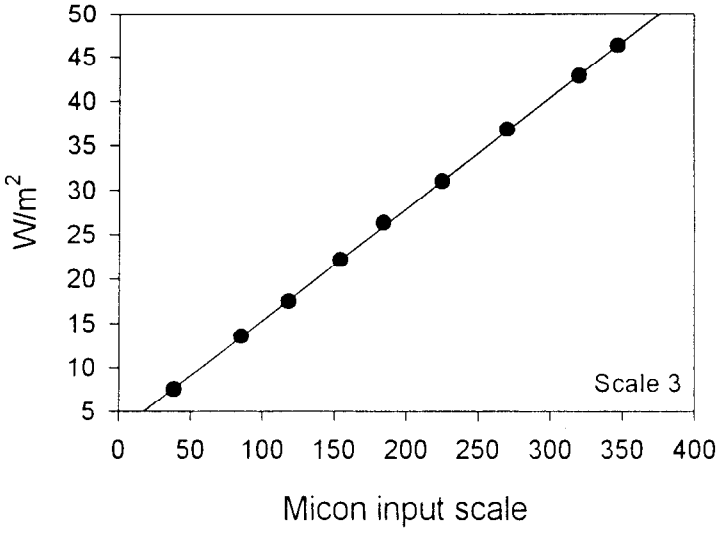

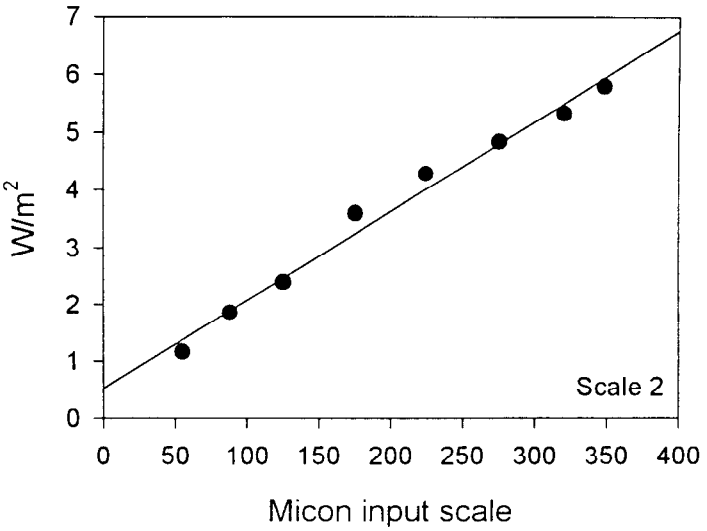

Figure 8 : Calibration plot for light sensor scale 2. (W/m^2= 0.555+0.0155* INPUT).

time, the previous set up was not available and it was re-calibrated on a lab bench using one lamp of the same type used in the bioreactor and another light sensor (ANRITSU NA-9422A) which measures the illumination in W/m^2 at 630 nm on its active surface. In both cases the light sensor used was able to measure the light coming only from one direction and therefore illumination conditions for the calibration were mono-dimensional.

The calibration obtained with this sensor, for each amplifier scale, can be found on that technical note. That is the calibration that has been used until now in the ESTEC bioreactor.

As it is now available in the laboratory a light sensor of the same model to the one that has to be re-calibrated, but which measures only in one direction, it is possible to use it to re-calibrate the bioreactor sensor. J. F. Cornet has checked with an spherical sensor that when using mono-dimensional illuminations, the light intensity measured by the spherical sensor in one point and the one measured by the flat one at the same place

Figure 9 : Calibration plot for light sensor scale 1. (W/m^2= 0.62+0.00193* INPUT).

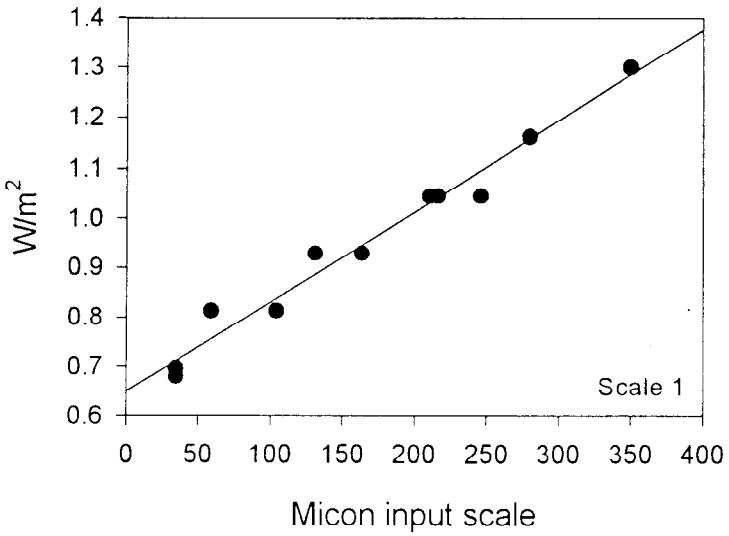

are equal. Therefore the available flat sensor was used to re-calibrate the spherical light sensor used in the bioreactor. The calibration procedure is described below and a summary of the steps followed can be found in table 4. The calibration of the sensor was done in a dark room and using the same lamps actually set up in the bioreactor. The calibration procedure was done in several steps. In the first step it was measured the light intensity in a surface at different distances from a light source, until a surface of 3x3 cm was obtained in which the light intensity measured at different points separated 1 cm apart, had a difference in light intensity smaller than 1 $\mu mol.m^{-2}.s^{-1}$. In this conditions the surface was considered homogeneous.

What is more, as a second condition the average values obtained on an equal surface positioned 1 cm behind the previous one had to have as an average, a value difference also smaller than 1 $\mu mol.m^2.s$. The values measured on this surfaces can be seen on table 3. In this conditions it was considered that the light intensity falling on the flat sensor surface and the spherical sensor were homogeneous enough for the calibration. Under this conditions a factor to relate the light measurements obtained by the flat sensor on the measurement surface and the readings obtained by the same sensor once it was attached to the spherical ball allowed to calculate a coefficient to convert the light intensity at the measuring sphere surface and the light intensity actually received by the sensor. With the obtained values a conversion factor of 97.36 was obtained. Once this factor is obtained it is possible to directly compare the readings of the two sensors attaching the ball to each of them and then, once both measurements are correlated, the real values at the ball surface can be obtained. This was done in a second step.

For the second step the ball of the detector was attached to the new factory calibrated sensor. The complete instrument was placed perpendicular to the light source in a dark chamber (mono-dimensional illumination). The distance of the sensor to the lamp was chosen so as to obtain, with one lamp, a range of light intensities covering all the four ranges of the span of the sensor to calibrate (0-400 W/m^2). Each light intensity corresponded to one voltage supplied to the lamp. For each voltage the light intensity measured by the sensor was recorded, and the values converted to the values at the ball surface by using the previously calculated coefficient. At this point it must be mentioned that the sensor used as a reference gives the light intensity values in $\mu mols.m^{-2}.s^{-1}$, and the needed values for the GPS are in W/m^2. The conversion between those values was done by multiplying the obtained values by a constant factor (1/4.95). This factor was obtained as explained in the corresponding light sensor manual (Biggs 1985) and was similar to the approximate conversion values given in the same manual for this type of lamps (1/4.6). The obtained values are in W/m^2 in the range of wavelengths between 400 and 700 nm. However the range considered in the Photosim simulator is of 350-750 nm. A correction for our halogen Sylvania lamps was found to be by J.F.Cornet of 1.8 to correct for this fact. Consequently this correction factor was also applied to the previously obtained values in order to adequate the readings to the ones needed by the model.

Once this values were obtained, the new sensor was removed from the ball, but without moving the ball from its place. At this point the sensor to calibrate, was attached to the light ball and the same light intensities as before (same voltages) were supplied. In this case the readings at the input of the MICON controller (4-20 mA) were converted by the MICON in a range of values between 0 and 400. This values, together with the scale used by the amplifier were recorded. Those measurements allowed to obtain a correlation between the light intensity at the ball surface, and the internal MICON scale.

Those correlations can be seen in figures 6, 7, 8, and 9. The equations of the linear regressions for each amplifier scale, were calculated and the parameters obtained can be found in the same figures. Those values were introduced in the MICON as a calibration scale.

To overcome the problem that appears when the light amplifier changes its scale from the second scale to the first one, and the input signal on the MICON falls to zero, a condition was set up in the MICON program so as always when the digital input corresponding to the first scale is ON, and the digital inputs corresponding to the third or fourth scale are also ON at the same time, then the MICON light reading is set to a fixed value that corresponds to the highest value of the first scale. This only happens momentarily when, as the light decreases, the light amplifier is momentarily changing from using the second scale to using the first scale.

STEP	ACTION TAKEN
1	Determination of the correction coefficient for the light collector ball effect.
2	Radiation measurement, in mono-dimensional illumination conditions using the reference sensor + light collector ball.
3	Determination of the radiation at the light ball collector surface from the sensor measured radiation, using coefficient obtained at step 1.
4	Conversion of the reference sensor radiation units ($\mu mol \cdot m^{-2} \cdot s^{-2}$) to $W \cdot m^{-2}$.
5	Correction for the wavelength measurement span of the sensors (400-700 nm) to the model ones (350-750 nm).
6	Micon input measurement at the same illumination conditions and voltages of step 2, using the sensor to calibrate +light collector ball.
7	Calculation of the correlation among the Micon input signal and the real radiation at the ball surface.

Table 4 : Summary of the different steps followed for the light sensor re-calibration.

HIGH DILUTION RATE TESTS

As mentioned in the introduction this tests have the objective to confront the actual mathematical model describing the growth of Spirulina in compartment IV, with data obtained at higher dilution rates than the ones used in previous validations. The values of the experimental variables fixed for this experiments were set according to the ones stated for high dilution rate tests in TN-24.2 .

For the tests the flow rate was set to the corresponding value and the input and output flows of the bioreactor were measured daily and corrected in case of deviation.

The light intensity values were obtained by manually fixing the output of the light intensity controller. The output control values were chosen to obtain a desired light intensity according to the function describing light intensity vs. output of the controller, that can be seen in figure 5.

Test A (0.025 h^{-1})

For this test the flow rate was set at 0.175 l/h which for our 7 litres working volume corresponds to a dilution rate of 0.025 h^{-1}. The residence time in this case is of 40 hours. The light intensities chosen for this tests were 100 W/m^2 for the low F_r and 200 W/m^2 for the high F_r. To check for the repeatability of the steady states the experiments were done twice.

The experiments were monitored by the measurements obtained with the on line probes as well as by external off-line analysis of samples taken manually. The off-line measurements consisted in total dry weight, total carbohydrates and protein measurements. To calculate the EPS from the total sugars present in the samples, it was assumed that the saccharides contained in the active biomass were the 15% of the total biomass according to TN 19.2. This amount was subtracted from the amount of total carbohydrates measured to obtain the amount of EPS. Total carbohydrates were measured by the phenol method. Total proteins were measured on a freeze dried sample

Figure 10 : Plot of the results obtained at D : 0.025 h^{-1} test A1.

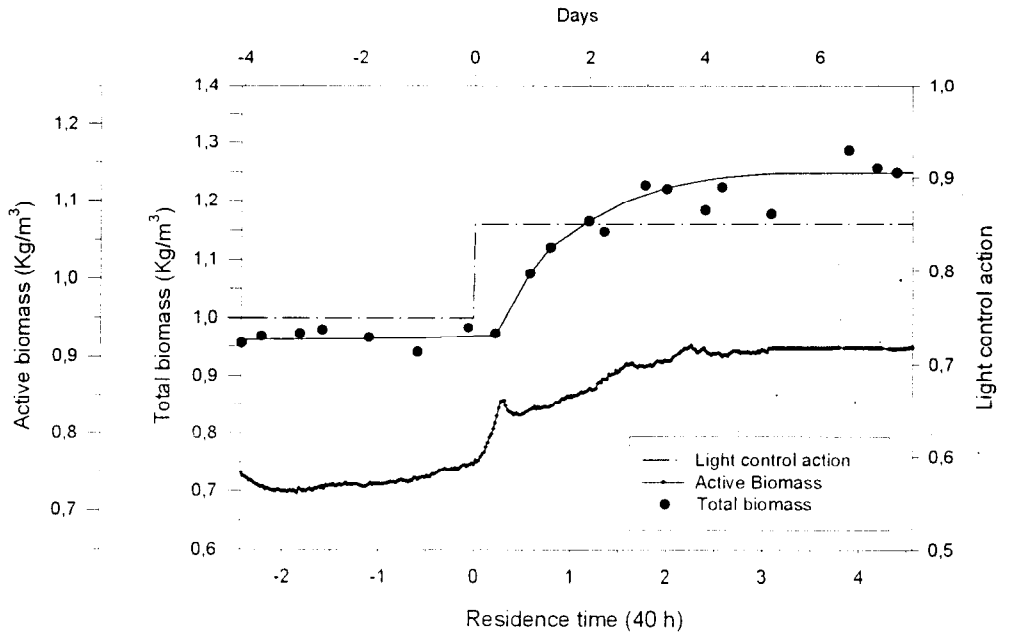

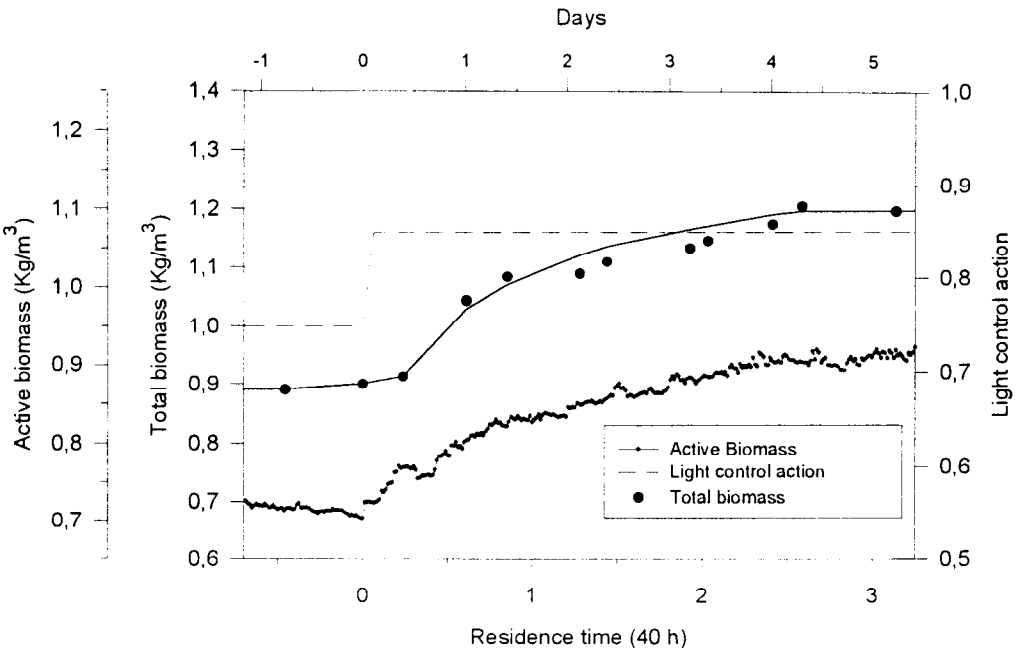

Figure 11 : Plot of the results obtained at D : 0.025 h^{-1} test A2.

by the Lowry method using BSA as standard. Total dry weight was measured by drying, at 95 °C triplicate filtered samples to constant weight.

The experiments begun by setting the flow (0.175 l/h) and a light intensity of 100W/m^2 and wating until the biomass concentration remained stable (phase A) At this point three different samples were taken at tree different times for the biomass composition analysis. After that the light intensity was changed to 200 W/m^2 and the new stabilisation of the biomass was attained (phase B) after some time. Once reached three more samples were taken and analysed.

Figure 12 : Plot of the simulation results obtained with Photosim for the conditions of this test (D : 0.025 h^{-1}.)

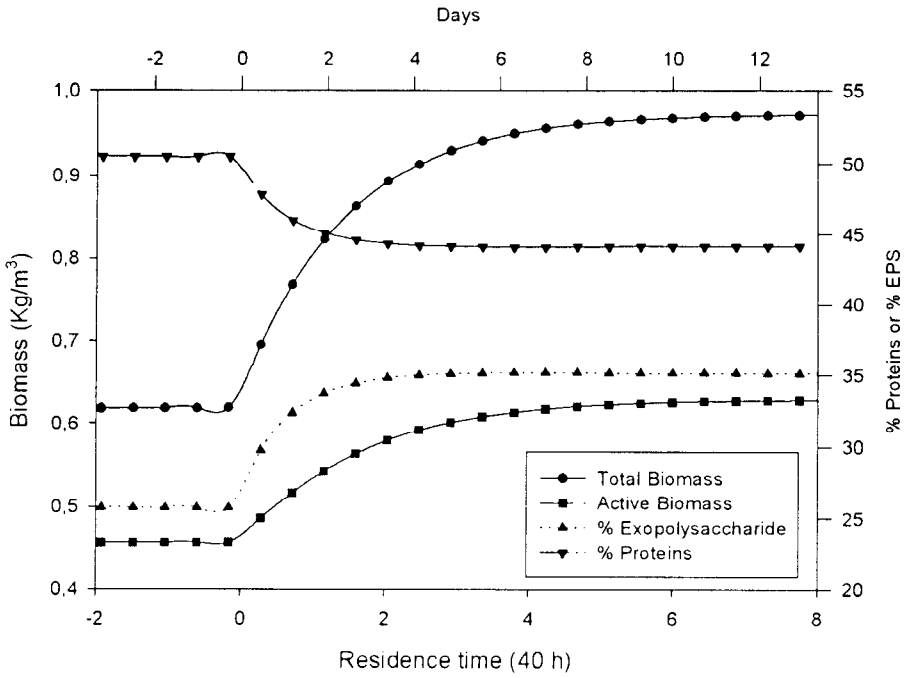

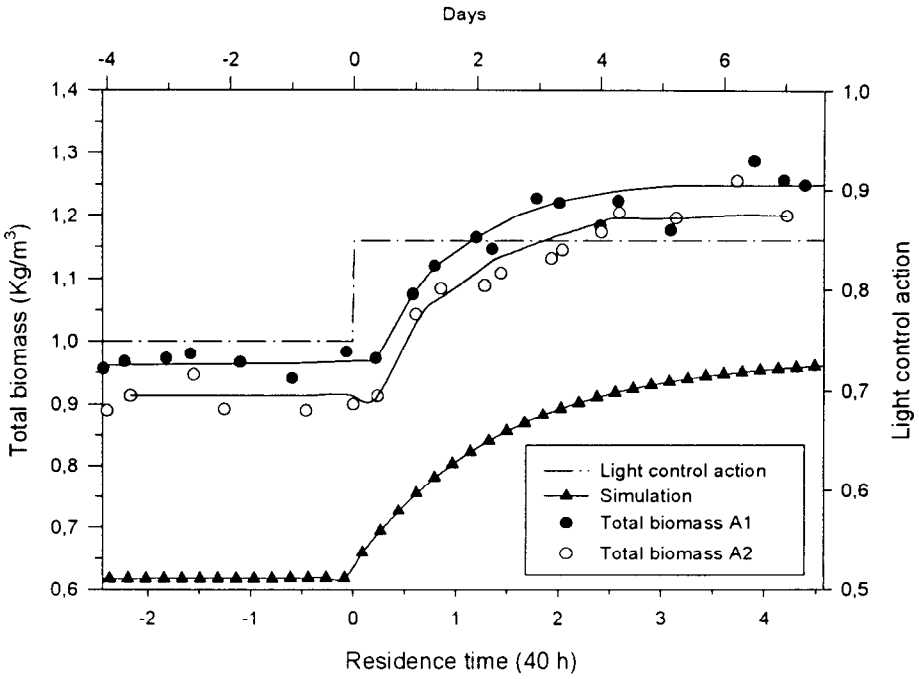

Figure 13 : Comparison of the total biomass experimental results obtained at D : 0.025 h^{-1} and the simulation results, for the tests A1 andA2.

Figure 10 shows the dynamic evolution of the biomass concentration for the first 0.025 h^{-1} dilution rate test. As an average the biomass changed from a total biomass concentration of 1 g/l to a 1.2 g/l . In figure 11 it can be seen the results of a duplicate of this test which shows a change from 0.91 to 1.13.

As an average we have therefore a change of about 18% in total biomass concentration. The measures done on the biomass concentration give the same values as an average (0.94 to 1.16). This is a small change and it would be desirable to perform

Figure 14 : Comparison of the active biomass experimental results obtained at D : 0.025 h^{-1} and the simulation results, for the tests A1 andA2.

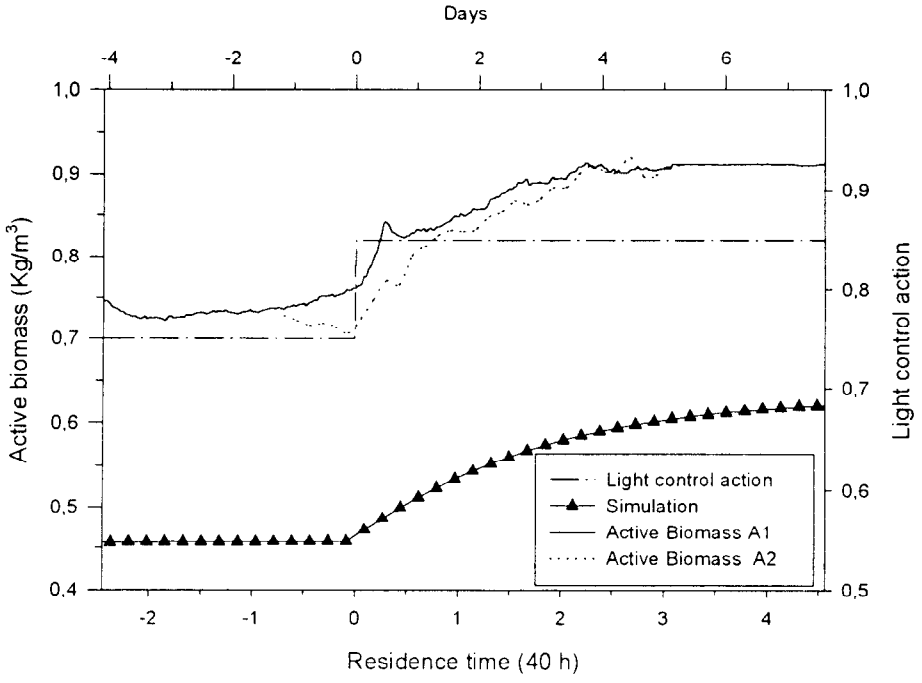

future tests between two light intensities with a bigger difference among them. Besides the increase in biomass concentration there is an increase in the exopolissaccharide content from about 23% to 37% as an average. This represents about a 36% of increase. The proteins measured showed as an average a decrease from 62% to 47% which is about a 24% of decrease.

The dyamic behaviour of the culture shows, as an average a 95% response time of around 3.5 days (85 h). A summary of the results can be seen in table 4. Those results can be compared with the predicted behaviour by the Photosim simulator Figures 12 13 and 14 .

The results given in table 4 were obtained by using the steady state solution for the given continuous culture conditions (Photosim option 7) .The dynamic behaviour was also simulated and can be seen in figure 12. The simulator gives a steady state solution lower than the obtained average results (0.61 to 0.97) for total biomass. However the predicted exopolysaccharide concentration is quite similar (26 to 35%). The 95 % response time on total biomass is however longer (6.9 days) than the real one. The biomass protein content changes from about 51% to 43% which can be considered in good agreement with the obtained results, given the usual precision of this kind of biochemical analysis (10-20%).

Table 5 : Summary of the results obtained during the tests done at 0.025 h^{-1}.

	A1 Phase a	A1 Phase b	A2 Phase a	a2 Phase b	Weighted Average Phase A	Weighted Average Phase B	Simulation Phase a	Simulation Phase b
Fr W/m^2	100	200	100	200	100	200	100	200
Total biomass (XT) Kg/m^3 +/- Std. Dev.	1.03 +/- 0.09	1.18 +/- 0.04	0.91 +/- 0.06	1.13 +/- 0.06	0.94 +/- 0.05	1.16 +/- 0.03	0.61	0.97
Active biomass (XA) Kg/m^3 +/- Std. Dev.	0.72 +/- 0.08	0.95 +/- 0.05	0.69 +/- 0.07	0.96 +/- 0.02	0.7 +/- 0.05	0.96 +/- 0.02	0.45	0.62
Spectrophotometer (XT) Kg/m^3 D.W (Kontron)	1.	1.1	1.2	1.3	1.1 +/- 0.07	1.2 +/- 0.14	-	-
Freeze dried (XT) Kg/m^3	0.91	1.16	0.98	1.17	0.94 +/- 0.05	1.16 +/- 0.01	-	-
Exopolysaccharide (EPS) % of XT +/- Std. Dev.	29.8 +/- 2.	36.8 +/- 4.	20.8 +/- 1.	28. +/- 10.	23 +/- 1	35. +/- 4	26	35
Proteins (P) % of XT +/- Std. Dev.	62. +/- 1.5	-	61.4 +/- 2	46.8 +/- 5.	62 +/-1.2	47 +/- 5	50.8	43.3

Test B (0.035 h^{-1})

For this test the flow was set at 0.245 l/h which for the 7 litres working volume corresponds to a dilution rate of 0.035 h^{-1}. The residence time in this case is of 28.6 hours. The light intensities chosen for this tests were the same as in the previous test. That is 100 W/m^2 for the low F_r and 200 W/m^2 for the high F_r. To check for the repeatability of the steady states the experiments were also done twice. The experiments were followed as in the previous case by the measurements obtained using the on line probes as well as by external off line analysis of manually taken samples. The off line measurements analysis were the same as in the previous case.

The steady state total biomass concentration (table 6) gives in this case lower concentrations than in the previous case due to the increase in the liquid flow rate. The total biomass values (figure 15,16) change from 0.66 to 0.9 g/l. This represents a decrease, compared to the previous dilution rate used, of about 30% in biomass concentration. The calculated active biomass concentrations were of 0.48 and 0.62 g/l respectively for each phase, which represents about a 33% decrease from the values obtained at the previous flow rate. The values of the exopolysaccharide obtained were similar to the ones measured in the previous dilution rate changing from 29 to 31 %. The protein measurements gave this time higher values than could be expected, according to the obtained exopolysaccharide measured. However they are inside the usual range of precision obtained for this kind of analysis. The 95% response time are around 2.5 days (60 h).

Comparison with the simulated values (figures 17, 18, 19 and table 6), obtained as in the previous case using option 7 of the simulator, allows to conclude that the simulated values are too low compared to the experimental ones. There is a 94 and 69 % difference between the real and the simulated total and active biomass values. This is a too big difference not to be attributed to any experimental error or deviation and indicates that the model should be updated for this situation. In this case the simulated 95% response times are around 6.9 days (169h) which also appears as a too long time.

Figure 15 : Plot of the results obtained at D : 0.035 h^{-1} test B1.

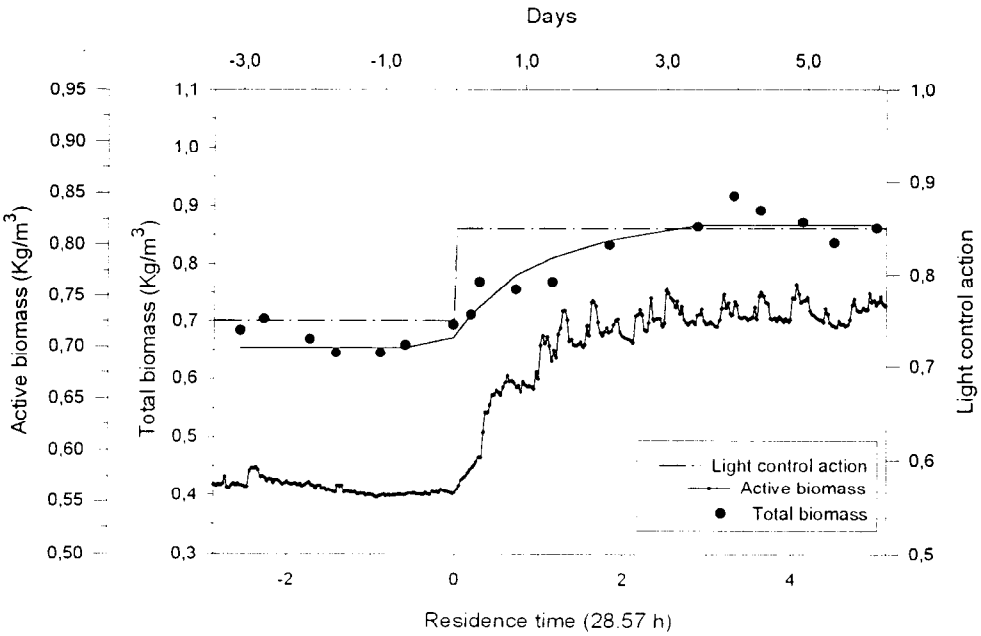

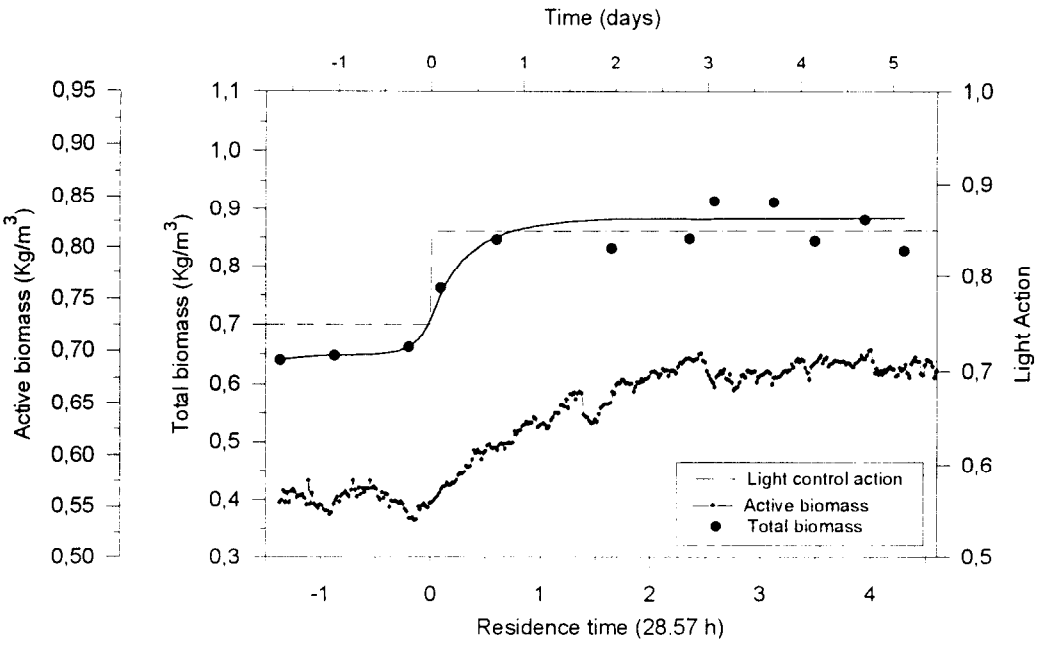

Figure 16 : Plot of the results obtained at D : 0.035 h^{-1} test B2.

The simulated exopolysaccharide values are higher than the measured ones but the usual low precision of this biochemical analysis, has to be considered in this case. The protein content measured was also higher than the simulated values.

Figure 17 : Comparison of the total biomass experimental results obtained at D : 0.035 h^{-1} and the simulation results, for the tests B1 andB2.

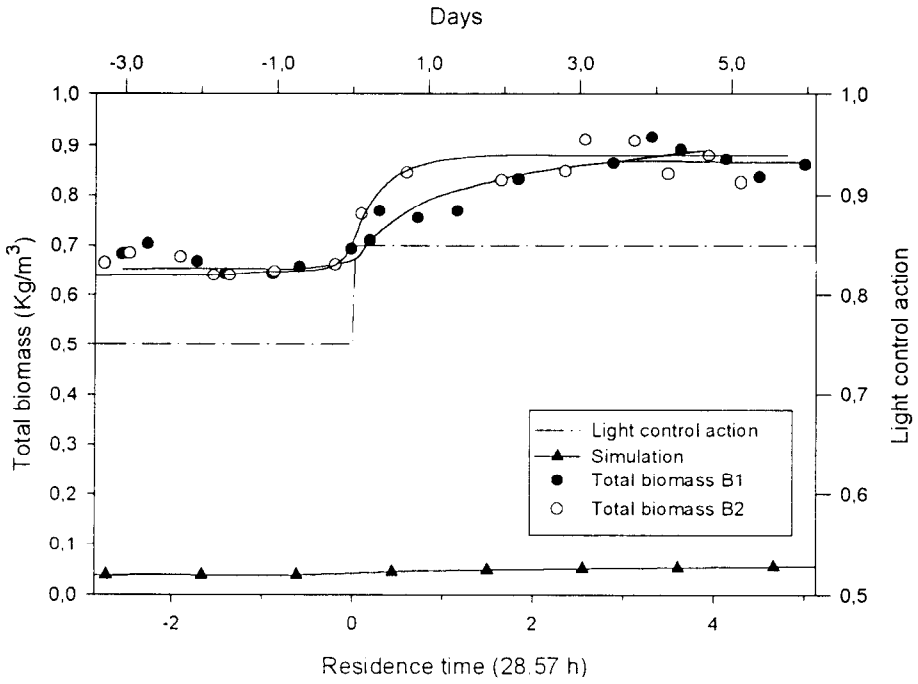

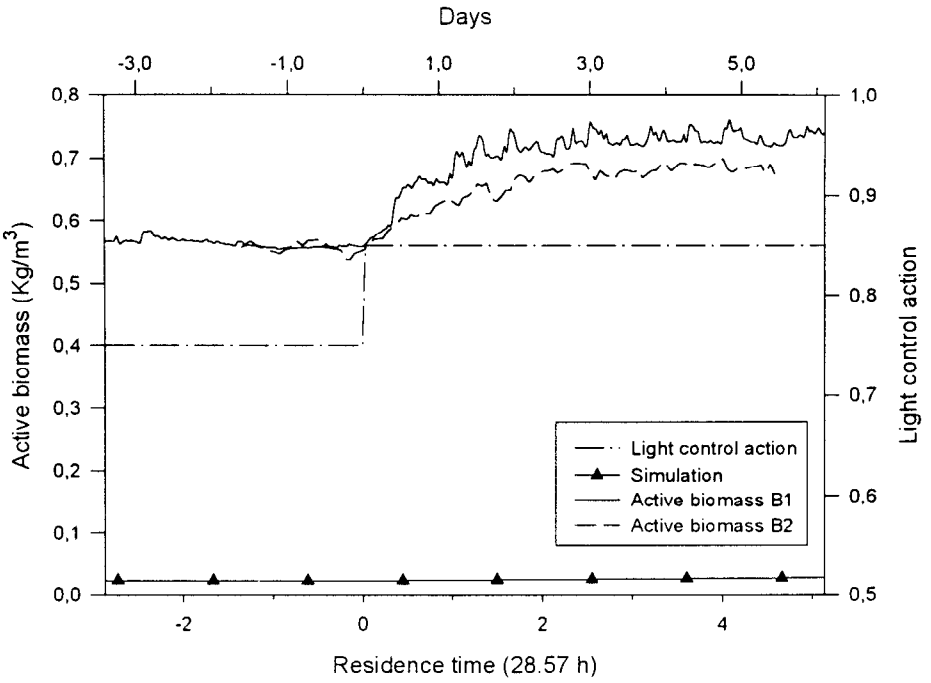

Figure 18 : Comparison of the active biomass experimental results obtained at D : 0.035 h^{-1} and the simulation results, for the tests B1 andB2.

Figure19 : Plot of the simulation results obtained with Photosim for the conditions of this test (D : 0.035 h^{-1}.).

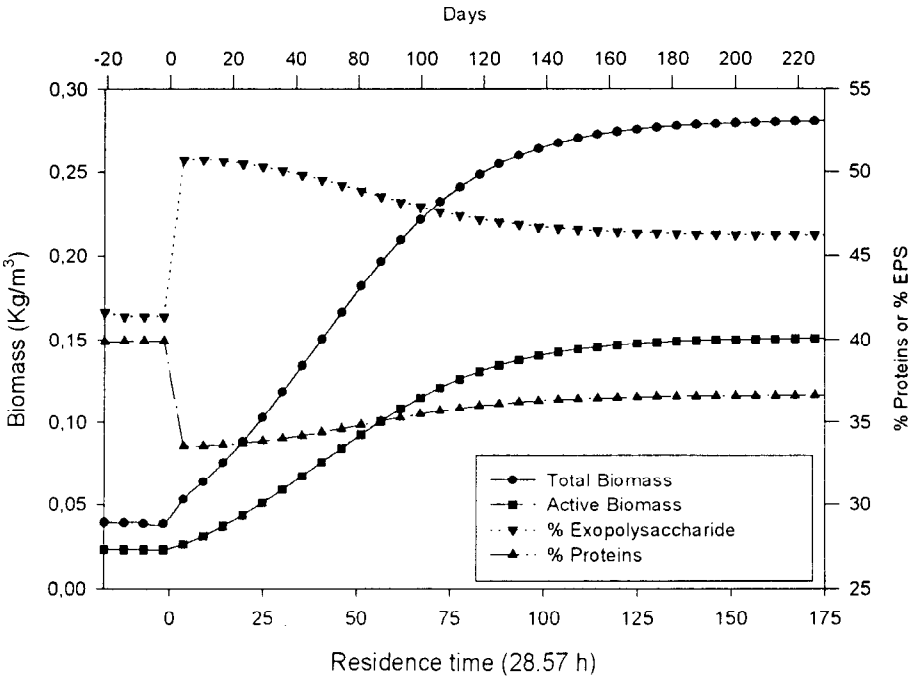

	B1 Phase a	B1 Phase b	B2 Phase a	B2 Phase b	Weighted Average Phase A	Weighted Average Phase B	Simulation Phase a	Simulation Phase b
Fr W/m^2	100	200	100	200	100	200	100	200
Total biomas (XT) Kg/m^3 +/- Std. Dev.	0.66 +/- 0.02	0.92 +/- 0.02	0.66 +/- 0.02	0.89 +/- 0.02	0.66 +/- 0.01	0.9 +/- 0.01	0.039	0.28
Active biomass (XA)Kg/m^3 +/- Std. Dev.	0.502 +/- 0.02	0.63 +/- 0.01	0.46 +/- 0.02	0.61 +/- 0.02	0.48 +/- 0.01	0.62 +/- 0.01	0.023	0.0.15
Spectrophotometer (XT) Kg/m^3 D.W (Kontron)	0.81	1.1	0.76	0.98	0.78 +/-0.03	1.0 +/-0.08	-	-
Freeze dried (XT) Kg/m^3	0.72	0.89	0.62	0.91	0.67 +/-0.07	0.9 +/-0.01	-	-
Exopolysaccharide (EPS) % of XT +/- Std. dev	25 +/- 20	31. +/- 1.6	30 +/-8.	32. +/-2.	29. +/-7	31 +/-1	41.3	45.9
Proteins (P) % of XT +/- Std. dev	52 +/-2	60 +/-3	66. +/-4	61. +/-5	54. +/-2	60. +/-3.	39.7	35.3

Table 6 : Summary of the results obtained during the tests done at 0.035 h^{-1}.

Model reconciliation

Experimental results were evaluated with the Clermont Ferrand simulation team and the ESA technical officer. As a conclusion, the most possible explanation for the observed effects at high dilution rate is that in high illumination conditions and low biomass concentrations, light might enter the previously considered dark area of the bioreactor. This efectively increases the working illuminated volume. New simulations were performed using a working illuminated volume of 65% instead of 52%. As can be seen in figures 20 and 21, the results show the agreement of the model with the observed experimental values.

Figure 20 : Comparison of the total biomass experimental results obtained at D : 0.025 h^{-1} and the simulation results with useful volume value set at 65% . (tests A1 andA2).

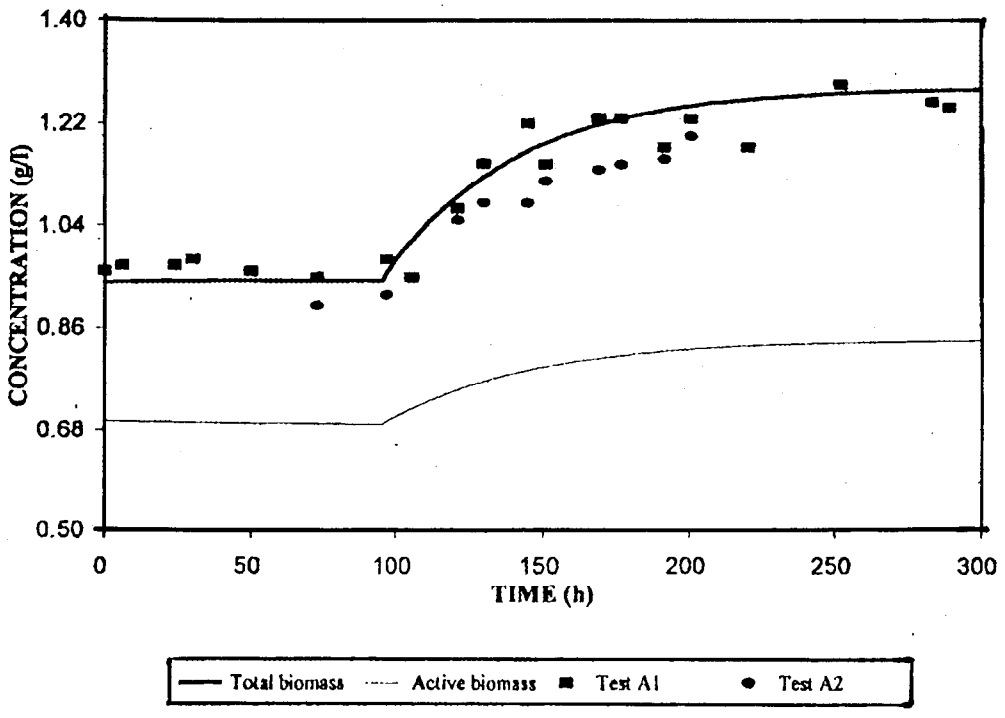

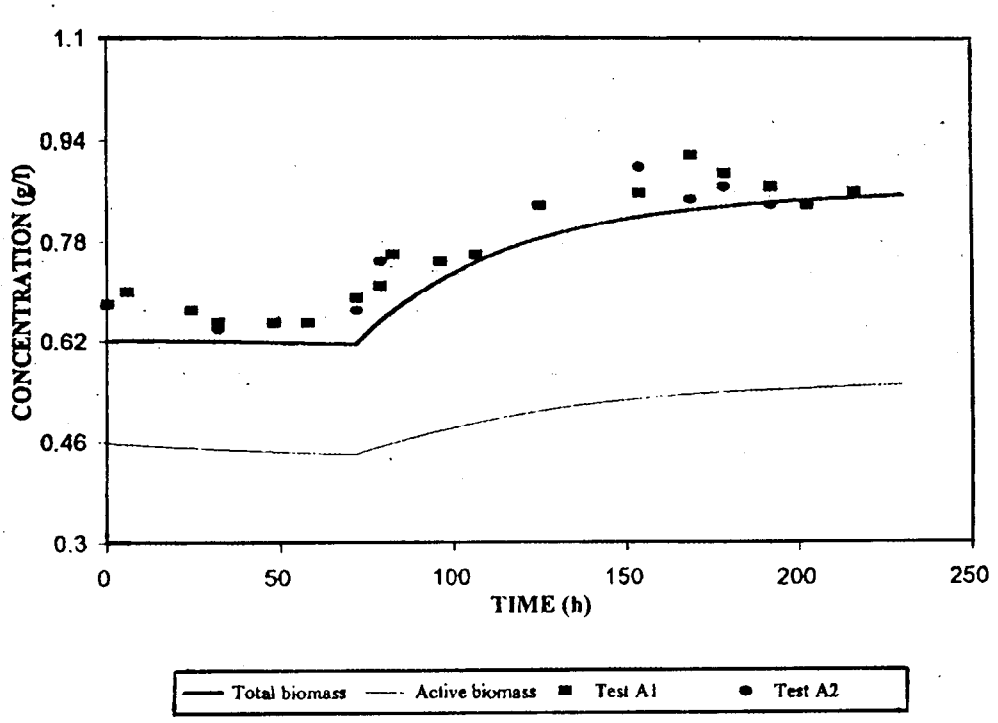

Figure 21 : Comparison of the total biomass experimental results obtained at D : 0.035 h^{-1} and the simulation results with useful volume value set at 65% . (tests B1 and B2).

REFERENCES

BINOIS C. (1994) Automatisation d'un Écosystème Artificiel Utilisé comme système de support vie. Première Interaction Modèle/Système de contrôle. ESTEC-ESA contract CCN5 Final Report.

BINOIS C. (1994) MELISSA Technical Note 18.2

BIGGS (1985) Radiation Measurement. in Li-COR Radiation Measurement Instruments. 20-24. Excerpted from : Advanced Agricultural Instrumentation. (1984) (Proc. NATO Adv. Inst. on Advanc. Agric. Instr.) W.G. Gensier (Ed.) M. Nijhoff Publish. Dordrecht The Netherlands.

CORNET J. F. ; DUSSAP C. G. ; GROSS J. B. (1993) Modelling of Physical Limitations in Photobioreactors. MELISSA Technical Note TN 19.1 .ESTEC-ESA contract PRF 130820

CORNET J. F. ; DUSSAP C. G. ; GROSS J. B. (1993) Modelling of Physical Limitations in Photobioreactors. MELISSA Technical Note TN 19.2 .ESTEC-ESA contract PRF 130820.

FULGET N. (1995) Study for the non linear Model Based Predictive Control of Spirulina compartment using knowledge model. Technical Note 24.2 ESTEC-ESA P.O..142356.

THAUVOYE O. (1994) Validation dun Modele Mathematique de Croissance de Bacteries Photosynthetiques en Photobioreacteur Cylindrique. ESTEC Working Paper ESA-X-1101.